De-biasing of the velocity determination for double station meteor observations from CILBO

Thomas Albin[1,2], Detlef Koschny[3,4], Gerhard Drolshagen[3], Rachel Soja[1], Bjoern Poppe[2] and Ralf Srama[1]

[1] **Institute of Space Systems, University of Stuttgart, Pfaffenwaldring 29, 70569 Stuttgart, Germany**
albin@irs.uni-stuttgart.de, soja@irs.uni-stuttgart.de, srama@irs.uni-stuttgart.de

[2] **Universitätssternwarte Oldenburg, Institute of Physics and Department of Medical Physics and Acoustics, Carl von Ossietzky University, 26129 Oldenburg, Germany**
bjoern.poppe@uni-oldenburg.de

[3] **European Space Agency, ESA/ESTEC, Keplerlaan 1, 2201 AZ Noordwijk ZH, Netherlands**
detlef.koschny@esa.int, gerhard.drolshagen@esa.int

[4] **Chair of Astronautics, Technical Univ. Munich, Boltzmannstraße 15, 85748 Garching, Germany**

The Canary Islands Long-Baseline Observatory (CILBO) has been in operation since the end of 2011 and continuously working since January 2013 (Koschny et al., 2013). CILBO consists of two cameras on the island of Tenerife (camera ICC7) and La Palma (ICC9). To date, approximately 12000 meteors have been simultaneously measured, allowing precise orbit reconstruction. Certain meteors like Perseids show mostly persistent trains or wakes that may cause a position determination bias in the software. Large and fast meteors decelerate significantly during their appearance and cause an additional observational bias possibly by saturation effects on the CCD chips. Here we analyze these biases in the CILBO data and determine whether orbit reconstructions need to be corrected as a function of velocity, brightness or meteor shower.

1 Introduction

The Canary Islands Long-Baseline Observatory (CILBO) has been operated continuously since January 2013. It observes meteors stereoscopically for precise orbit determination. Two similarly built cameras are installed on the islands of La Palma and Tenerife, and are named ICC9 and ICC7, respectively. ICC9 (aimed eastwards) and ICC7 (aimed westwards) can be seen in *Figure 1*. The overlapping area of both cameras at an altitude of 100 km is approximately 3000 km^2 (Drolshagen and Ott, 2014). An additional camera, named ICC8 is installed next to ICC7 on Tenerife for meteor spectroscopy.

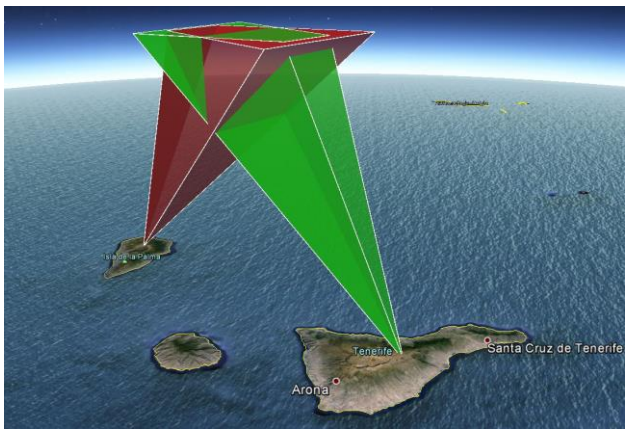

Figure 1 – Field of View (FOV) of both CILBO cameras (La Palma: ICC9, Tenerife: ICC7). The FOV data have been obtained from Koschny 2015 (priv. comm.).

A detailed description of the camera system is given in Koschny et al. (2013), and Koschny et al. (2015) provide the current status of ESA´s Meteor Research Group (MRG) working on the CILBO system. Drolshagen et al. (2014) and Ott et al. (2014) describe first scientific results regarding the velocity and mass distribution, respectively. Further scientific analysis is given by Drolshagen et al. (2015) and Kretschmer et al. (2015). A detailed analysis of the observation biases is found in Albin et al. (2015). The work describes a bias dependent on the camera pointing, such that the eastwards aligned camera ICC9 detects fainter states of meteors. Furthermore, the CCD sensitivity and signal loss is magnitude-dependent.

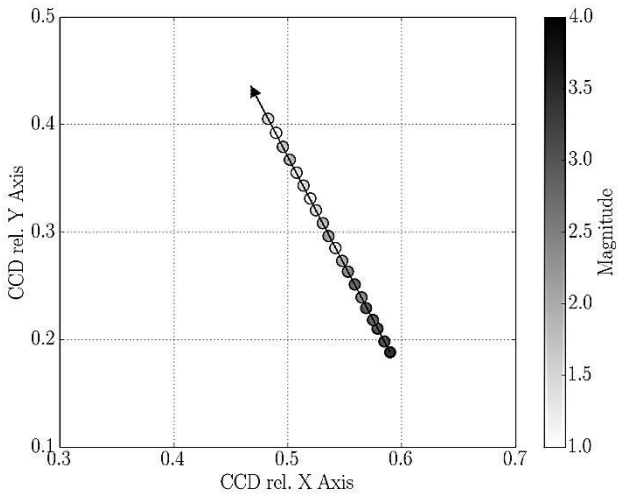

Figure 2 – Meteor trail of a meteor captured on ICC9 (2014-06-07/215740.daf). The arrow indicates the flight path. X and Y axis show the CCD coordinates and the dots are the determined photometric centers. The gray scale indicates the measured brightness in magnitude.

This work focuses on a possible velocity determination bias. CILBO currently uses MetRec (Molau, 1999) as the detection software for both cameras with identical settings. Each 40 ms long video frame is analyzed by this

software package. If a meteor's brightness triggers the software detection threshold, it determines the photometric center of the meteor on each frame and saves the corresponding position data in a file. These files are then used by the MOTS software (Koschny and Diaz, 2002) to determine if meteors have been simultaneously detected by both cameras. The determined values (velocity, position, etc.) are then saved in a detailed altitude file (daf). An example of a detected meteor is shown in *Figure 2*.

2 Velocity bias

Very bright meteors (bolides), or meteors with slow angular velocities and consequently long pixel dwell times can overexpose the illuminated pixels. This glaring can cause negative side-effects like blooming or smearing during the image read-out, which may lead to a biased computation of the photometric center.

In this section we analyze whether the velocity determination is biased by the mentioned effects. For this analysis we use the data of 11785 meteors in the CILBO database.

The data set provides two velocity determinations: the actual physical speed in km/s and the velocity along the CCD chip in U/s. 1 U is the height of the CCD. Since the CCD has a resolution of 576 x 768 pixels the width values need to be normalized by a factor of 0.75. Considering the Field-of-View of CILBO (28 x 22 deg^2) these velocities can be transformed into an angular velocity in deg/s.

The main scientific objective of CILBO is to determine precise orbital elements of each stereoscopically observed meteor. For this computation, state vectors of each meteor are needed, consisting of three position and three velocity coordinates in km and km/s respectively. Therefore, in the following we will consider the physical velocity data only.

The yearly occurring Perseids cause mostly persistent trains that may cause an additional bias in the determination of the photometric center. We therefore produce two data subsets that are analyzed separately. The "Non-Perseids" subset consists of the data outside of the Perseids activity interval (21 July – 23 August), while the "Perseids" subsets contains the data inside this timeframe. A more differentiated stream associated analysis would require a proper orbit computation of each meteor. Currently these data are not available and the orbit computing algorithms are developed. Thus, we only differentiate between the Perseids and Non-Perseids to avoid further data filtering bias.

To analyze the velocity dependence on the captured video frame, the used data points are obtained from n+1 video frames. Here n is the number of detected velocity data points, since the velocity can only be computed by comparing 2 consecutive video frames. The first captured video frame is labeled with a 0. To interpolate the velocities between the image frames we use Gaussian Process (GP) algorithms implemented in the Python software library "Scikit" (Pedregosa et al., 2011). A detailed mathematical description can be found in Vanderplas et al. (2014) for astronomical applications. Section 5.4.3 of Rasmussen and Williams (2006) provides an extensive theoretical background and additional data applications.

In order to determine any bias in the velocity determination, other sources of differences between the data sets must be removed resulting in the need to be divided into further sub-sets. First, the data sets are sorted according to the number of video frames, so that meteors of the same trail length are used. Additionally these data are then divided into velocity ranges in the km/s and U/s domain to determine whether meteors with a slow angular velocity but the same physical speed are detected differently. Finally, the data are then sorted into maximum brightness intervals. This data sorting and filtering may lead to very small sub sets impairing the statistics. Thus, we only consider a few sets for which we have sufficient data. More data will therefore allow a more detailed and sophisticated analysis to be performed.

Non-Perseids

This section considers the whole data set outside the Perseid activity time interval (21 July – 23 August). All figures show the data points and standard deviation. The velocity profiles have been computed using a GP fit. This fit shows the expected mean velocity curve within a 95% confidence interval (gray area). *Figure 3a* shows the velocity of 12 meteors captured on 16 video frames. The initial velocity is 30 – 40 km/s and the maximum brightness range is 0.0 – 2.0 mag. It can be seen, that the mean velocity appears constant over around 11 frames. Afterwards the velocity decreases from around 34 km/s to 28 km/s within a few frames.

A similar but less significant velocity profile can be seen in figure 3b and 3c. Here, 9 and 10 frame long meteors have been extracted from the CILBO database. The shown meteors are fainter (2.0 – 4.0 mag) but have the same initial velocity as shown in figure 3a. The velocity drop at the end of the recorded frames is between 5 – 10%.

However, in some cases (meteors appearing on different long video recordings) "bell-shaped" velocity structures are present within the sub data set of bright meteors (*Figure 4*). The GP computed mean velocity within the confidence interval increases until frame number 4 and decreases afterwards. Although the fit curve shows a clear profile structure for the mean velocity values, the large error bars still lead to a high variation and possible misinterpretation of the data set.

The bell-shaped structure is more evident for fast and very bright meteors – namely bolides with a maximum brightness smaller than 0 mag. *Figure 5a – 5c* show the velocity curves of fast (54 – 64 km/s) bolides captured on

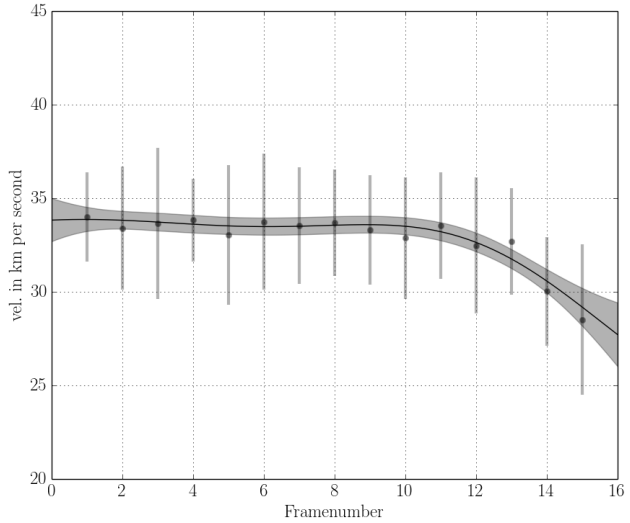

Figure 3a – Velocity in km/s vs. the video frame number n. n=0 is the inital video frame. The initial velocity range is 30 – 40 km/s and 0.0 – 0.25 U/s. 12 Non-Perseids, captured on 16 frames. The maximum brightness range is 0.0 – 2.0 mag.

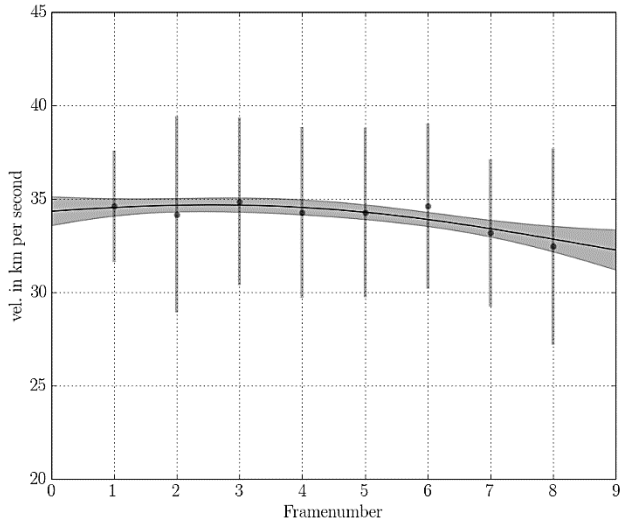

Figure 4b – Velocity in km/s vs. the video frame number n. n=0 is the inital video frame. The initial velocity range is 30 – 40 km/s and 0.0 – 0.25 U/s. 52 Non-Perseids, captured on 9 frames. The maximum brightness range is 2.0 – 4.0 mag.

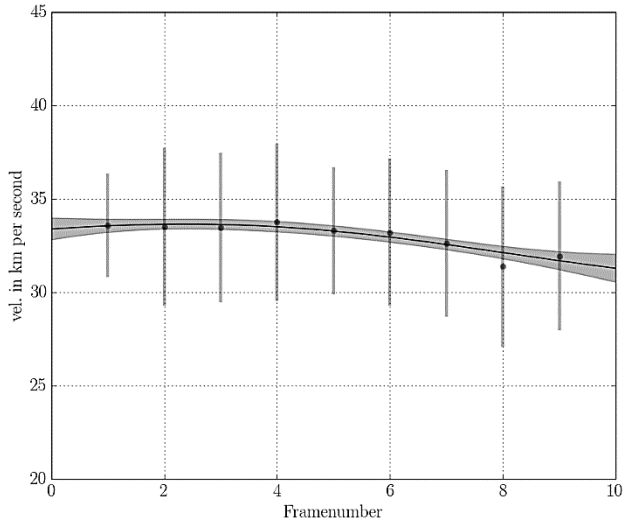

Figure 5c – Velocity in km/s vs. the video frame number n. n=0 is the inital video frame. The initial velocity range is 30 – 40 km/s and 0.0 – 0.25 U/s. 43 Non-Perseids, capured on 10 frames. Same brightness range as in b.

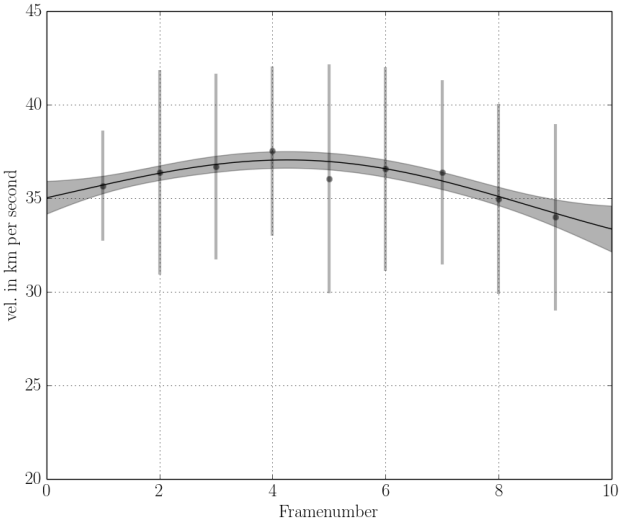

Figure 6 – Velocity in km/s vs. the video frame number n of 17 Non-Perseids, captured on 10 frames. Same parameter range as shown in *Figure 3a.*

7, 8 and 9 frames, respectively. All three plots show the bell-shaped velocity profile with a rather wide confidence interval due to the small number of meteors within the data set.

Perseids

For the Perseid analysis only data within the time interval 21 July – 23 August were used. The detailed altitude files do not save the meteor shower association for individual meteors. Therefore, the physical parameters were used to distinguish between the Perseid shower and sporadics. Specifically, Perseid meteors are defined using the activity time frame and the expected velocity range (here: 54 – 64 km/s).

Figure 6 shows the velocity profile of 3 Perseid bolides recorded on 9 video frames. The GP fit and its corresponding confidence interval show that in average the velocity increases until video frame 5 and decreases thereafter.

Similar bell-shaped velocity profiles are present within the Perseid data set, for both bright and faint meteors. The profiles appear similar to those seen in *Figure 4 and 5a – 5c*.

Software determination bias

The shown plots may result from physical processes and software depending bias. *Figure 3a – 3c* show a deceleration effect. The constantly appearing velocity drops to the end of the recorded video frames. Especially *figure 3a* shows a drop from around 34 km/s to 28 km/s after frame 11. This may result from atmospheric drag. This drag increases with lower altitudes due to the increasing air density. The force is linearly proportional to the cross sectional area of an object. Fainter meteors are caused by smaller meteoroids, which have smaller cross sections that lead to weaker atmospheric drag. This may explain the less significant velocity drop shown in *Figure 3b and 3c*. However, currently we did not yet

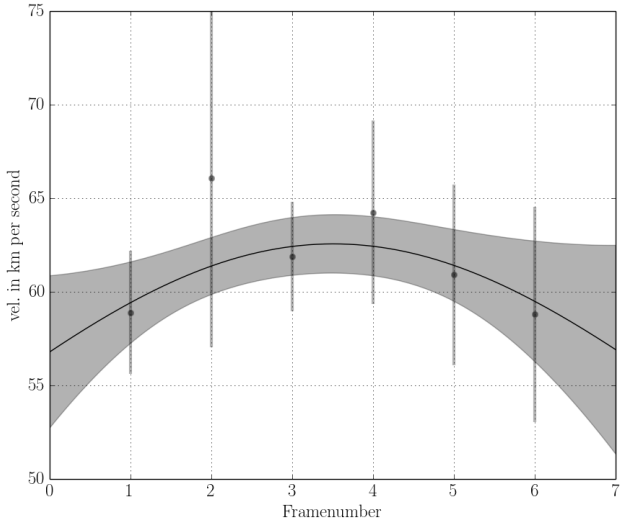

Figure 7a – Velocity in km/s vs. the video frame number n. n=0 is the inital video frame. The initial velocity range is 54 – 64 km/s and 0.0 – 1.0 U/s. The maximum brightness range is -10.0 – 0.0 mag. 7 Non-Perseids, captured on 7 frames.

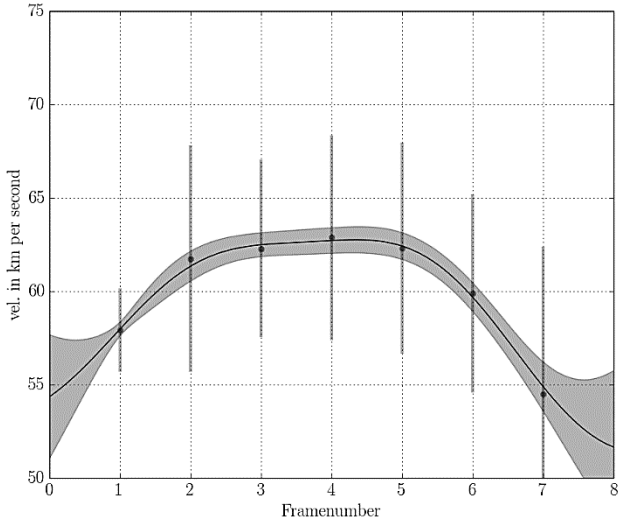

Figure 8b – Velocity in km/s vs. the video frame number n. n=0 is the inital video frame. The initial velocity range is 54 – 64 km/s and 0.0 – 1.0 U/s. The maximum brightness range is -10.0 – 0.0 mag. 12 Non-Perseids, captured on 8 frames.

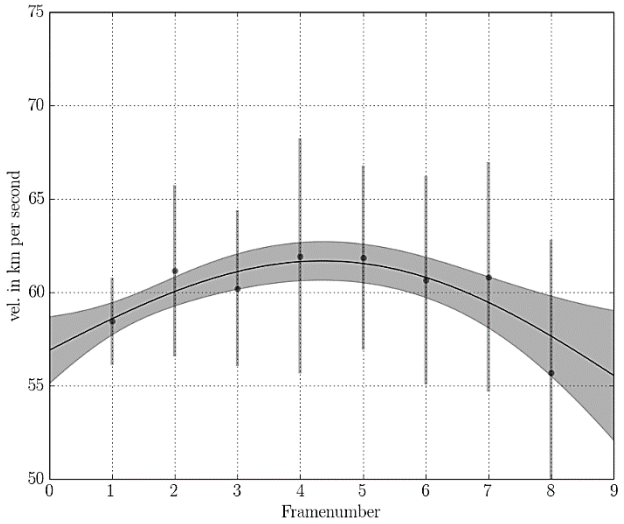

Figure 9c – Velocity in km/s vs. the video frame number n. n=0 is the inital video frame. The initial velocity range is 54 – 64 km/s and 0.0 – 1.0 U/s. The maximum brightness range is -10.0 – 0.0 mag. 10 Non-Perseids, captured on 9 frames.

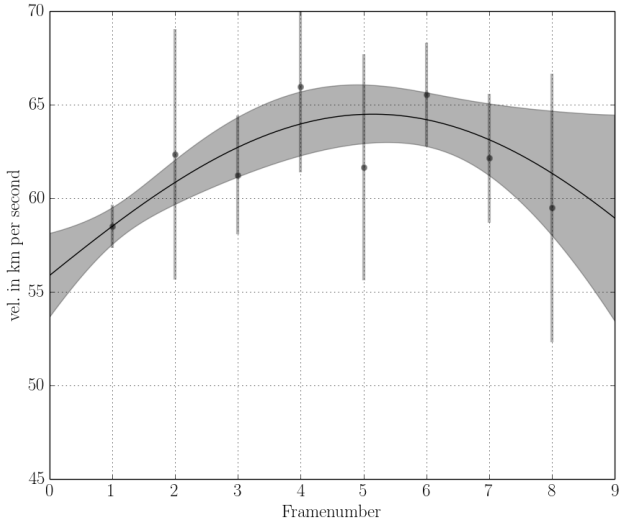

Figure 10 – Velocity in km/s vs. the video frame number n of 3 Perseids captured on 9 frames. n=0 is the inital video frame. The initial velocity range is 54 – 64 km/s and 0.0 – 1.0 U/s. The maximum brightness range is -10.0 – 0.0 mag.

analyzed the according video recordings. A position determination bias by the detection software cannot be excluded.

Figure 4 (0.0 – 2.0 mag meteors), *Figure 5a – 5c* (Bolides, brighter than 0 mag) and *Figure 6* (Perseid Bolides) show a bell-shaped velocity profile which cannot be explained by physical processes. We expect that pixels of the CCD camera are saturated due to the very large brightness maxima during the atmospheric entry. This leads to blooming and smearing effects on the CCD chip. The meteor broadens and appears wider on the chip with saturated pixels in the center. Our assumption is that these effects lead to an incorrect determination of the photometric center. Possibly the computed center shifts to the front of the meteor. This leads to higher distances of two determined centers on two consecutive video frames resulting in a higher velocity. After the brightness maximum the over saturation drops and leads again to correct computations. This effect may also be present in fainter meteors with low angular velocities (*Figure 4*). A smaller angular velocity leads to a longer pixel dwell time during the 40 ms exposure time. The pixels can saturate if the meteor reaches a certain brightness threshold at a certain angular velocity. This may lead to an incorrect position determination by the detection software.

3 Summary and outlook

We have presented a selection of velocity profiles for CILBO meteors for different numbers of video frames, initial velocities and brightness. This subgroup of the originally data set of 11785 meteors leads in some cases to poor statistics due to an insufficient number of meteors. A meteor stream differentiation would lead to worse, unusable statistics. However, we expect a major difference in the determination of the photometric center for meteors which show a wake. As the Perseids are the most likely candidates for this behavior, we analyzed them separately. The input data for this paper did not have stream information readily available, this exclusion

was performed by considering the Perseids activity time interval from 21. July to 23. August and the expected velocity range. Note that other streams showing wakes, like the Geminids, were not present in the data due to bad weather conditions. An improvement of the data analysis would be to use a proper stream allocation. These sub sets have been divided using the physical properties of the Perseids (velocity) and the activity time frame. In the "Non-Perseids" data set we found evidence for atmospheric deceleration, however wrongly determined meteor position cannot be excluded. Additionally, some meteors have bell-shaped velocity profiles that may result from CCD blooming and smearing. This affects bright meteors in particular. We suppose, that this results in an incorrect determination of the meteor position on the CCD. *Figure 4* might indicate this bell-shaped profile for fainter meteors. However, the error bars are rather large due to the chosen wide initial velocity range (30 – 40 km/s). More meteor observations will improve the statistical analysis and allow more detailed analyses. Additionally, we plan to analyze certain "bell-shaped" velocity profile meteors on the actual captured recordings.

Bright, and in some cases even fainter, Perseids show the bell shape profiles. To avoid any bias which is due to the determination of the photometric center, a different position determination method should be implemented in the detection software. For example, a Gaussian fit only to the front end (in the direction of flight) of the meteor image would avoid any shift of the position due to the development of a wake, as described in Koschny and Mc Auliffe (2006). Perseids cause mostly a bright persistent train behind the meteor wake. We therefore expect a shift in the determination of the meteor position on the CCD, resulting in a velocity decrease. However, this effect could not be identified in any Perseid sub set yet and also will be subject to further investigations.

Unbiased velocity vectors of meteors are necessary to compute precisely the corresponding orbital elements. Thus we will determine which velocity vector determination "strategy" is suitable for our data set to obtain high precision orbits. Such strategies may include using only half of the recorded frames to avoid velocity bias due to the strong velocity drop at the end of a meteor's appearance.

Additionally, theoretical modeling and analysis of the whole meteor detection (electronics and software) chain may improve our understanding of the data presented here.

References

Albin T., Koschny D., Drolshagen G., Soja R., Srama R. and Poppe B. (2015). "Influence of the pointing direction and detector sensitivity variations on the detection rate of a double station meteor camera". In Rault J.-L. and Roggemans P., editors, *Proceedings of the International Meteor Conference*, Mistelbach, Austria, 27-30 August 2015. IMO, pages 225–231.

Drolshagen S., Kretschmer J., Koschny D., Drolshagen G. and Poppe B. (2015). "Mass accumulation of Earth from interplanetary dust, meteroids, asteroids and comets". In Rault J.-L. and Roggemans P., editors, *Proceedings of the International Meteor Conference*, Mistelbach, Austria, 27-30 August 2015. IMO, pages 219–224.

Drolshagen E. and Ott T. (2014). "Meteoroid flux and velocity determination using image intensified video camera data from the CILBO double station". Bachelor thesis, unpublished.

Drolshagen E., Ott T., Koschny D., Drolshagen G. and Poppe B. (2014). "Meteor velocity distribution from CILBO double station video camera data". In Rault J.-L. and Roggemans P., editors, *Proceedings of the International Meteor Conference*, Giron, France, 18-21 September 2014. IMO, pages 16–22.

Kretschmer J., Drolshagen S., Koschny D., Drolshagen G. and Poppe B. (2015). "De-biasing CILBO meteor observational data to mass fluxes". In Rault J.-L. and Roggemans P., editors, *Proceedings of the International Meteor Conference*, Mistelbach, Austria, 27-30 August 2015. IMO, pages 209–213.

Koschny D. and Diaz del Rio J. (2002). "Meteor Orbit and Trajectory Software (MOTS) – Determining the Position of a Meteor with Respect to the Earth Using Data Collected with the Software MetRec". *WGN, Journal of the IMO*, **30**, 87–101.

Koschny D. and Mc Auliffe J. (2006). "Meteor orbit determination – points to be considered". In Mc Auliffe J. and Koschny D., editors, *Proceedings of the first EuroPlaNet workshop on meteor orbit determination*, Roden, The Netherlands, 11 - 13 September 2006, pages 85 – 94.

Koschny D., Bettonvil F., Licandro J., v. d. Luijt C., Mc Auliffe J., Smit H., Svedhem H., de Wit F., Witasse O. and Zender J. (2013). "A double-station meteor camera setup in the Canary Islands – CILBO". *Geosci. Instrum. Method. Data Syst*., **2**, 339–348.

Koschny D., Albin T., Drolshagen E., Drolshagen G., Drolshagen S., Koschny J., Kretschmar J., van der Luijt C., Molijn C., Ott T., Poppe B., Smit H., Svedhem H., Toni A., de Wit F. and Zender J. (2015). "Current activities at the ESA/ESTEC Meteor Research Group". In Rault J.-L. and Roggemans P., editors, *Proceedings of the International Meteor Conference*, Mistelbach, Austria, 27-30 August 2015. IMO, pages 204–208.

Molau S. (1999). "The Meteor Detection Software MetRec". In Arlt R. and Knoefel A., editors, *Proceedings of the International Meteor Conference*, Stara Lesna, Slovakia, 20 - 23 August 1998. IMO, pages 9–16.

Ott T., Drolshagen E., Koschny D., Drolshagen G. and Poppe B. (2014). "Meteoroid flux determination using image intensified video camera data from the CILBO double station". In Rault J.-L. and Roggemans P., editors, *Proceedings of the International Meteor Conference*, Giron, France, 18-21 September 2014. IMO, pages 23–29.

Pedregosa F., Varoquaux G., Gramfort A., Michel V., Thirion B., Grisel O., Blondel M., Prettenhofer P., Weiss R., Dubourg V., Vanderplas J., Passos A., Cournapeau D., Brucher M., Perrot M. and Duchesnay E. (2011). "Scikit-learn: Machine Learning in Python". *Journal of Machine Learning Research*, **12**, 2825–2830.

Vanderplas J. T., Connolly A. J., Ivezic Z. and Gray A. (2012). "Introduction to astroML: Machine learning for astrophysics". *Conference on Intelligent Data Understanding (CIDU)*. October 2012, pages 47–54.

Vanderplas J. T., Connolly A. J., Ivezic Z. and Gray A. (2014). "Statistics, Data Mining and Machine Learning in Astronomy". In Princeton University Press. Princeton, NJ.

The author, *Thomas Albin*, during his lecture (Photo by *Axel Haas*).